Geoderma 306 (2017) 40–49

Contents lists available at ScienceDirect

Geoderma

journal homepage: www.elsevier.com/locate/geoderma

Bulk optical characterization of dissolved organic matter from semiarid wheat-based cropping systems

Carlos M. Romero[a,*], Richard E. Engel[a,*], Juliana D'Andrilli[a], Chengci Chen[b], Catherine Zabinski[a], Perry R. Miller[a], Roseann Wallander[a]

[a] Land Resources and Environmental Sciences, Montana State University, 334 Leon Johnson Hall, Bozeman, MT, 59717-3120, United States
[b] Eastern Agricultural Research Center, Montana State University, 1501 North Central Avenue, Sidney, MT, 59270, United States

ARTICLE INFO

Keywords:
Semiarid soil
Winter wheat
Conservation agriculture
Excitation emission matrix
Parallel factor analysis

ABSTRACT

Dissolved organic matter (DOM) plays a critical role in the cycling of nutrients and long-term agricultural sustainability. The composition of DOM in soil is likely altered due to management, yet there is limited knowledge on the effect of long-term cropping on DOM chemical character. Here, we characterized water extractable DOM composition along a gradient of soil organic carbon (SOC) affected by differing cropping and tillage intensity in a semiarid climate of the northern Great Plains, USA. Soil samples (0–10, 10–20, 20–30 cm) were collected from conventional till-fallow winter wheat (*Triticum aestivum* L.; F_{till}-W), no-till spring pea/oilseed-wheat (*Pisum sativum* L.; P_g/O-W), and no-till continuous wheat (W-W) fields, and analyzed using UV/Vis absorbance and excitation-emission matrix fluorescence spectroscopy. The concentration of DOM decreased with depth and was significantly greater ($P < 0.05$) under W-W or P_g/O-W than F_{till}-W. The absorbance at 254 nm (Abs_{254}), a proxy for DOM aromatic nature, indicated that aromaticity decreased with depth and lower biomass-C inputs (i.e. W-W ≥ P_g/O-W ≥ F_{till}-W). Multidimensional parallel factor (PARAFAC) analysis revealed humic-like (C1, C2), monolignol-like (C3), and protein/tannin-like (C4) components with varying fluorescence intensities as a function of cropping system and soil depth. DOM humification, indicated by the humification index (HIX), increased significantly with depth ($P < 0.05$) and was higher for F_{till}-W (2.95) than W-W (2.61) or P_g/O-W (2.28). Overall, DOM became depleted of plant-derived constituents and was enriched by more decomposed, condensed substances in F_{till}-W, as compared to W-W or P_g/O-W soils. DOM composition is strongly affected by cropping intensity and such changes are important drivers controlling SOC accretion in arable soils.

1. Introduction

Dissolved organic matter (DOM) is the most dynamic and reactive component of soil organic carbon (SOC) in terrestrial ecosystems (Bolan et al., 2011). Although this pool accounts for a minimal portion of SOC (i.e. < 0.5–1%), DOM components exert a critical control over the biogeochemistry of soils by serving as a substrate for microbial activity and influencing the availability of plant nutrients and metal ions (Kalbitz et al., 2000; Bolan et al., 2011). The occurrence of DOM in soil is also critical to regulate both CH_4 and N_2O production (Bolan et al., 2011). Furthermore, terrestrial DOM is an important source of organic matter in freshwater ecosystems, affecting drinking water supplies through eutrophication and nutrient runoff (Wilson and Xenopoulos, 2009).

DOM is a heterogeneous mixture of plant and microbial derived constituents with varying degrees of reactivity (Bolan et al., 2011). Chemically, DOM can be conceptualized in terms of biologically active and stable humified fractions. Biologically active compounds are both aliphatic (i.e. amino acids, carbohydrates) and aromatic constituents (i.e. fulvic acids) of low molecular weight rapidly metabolized by soil microorganisms (Vázquez et al., 2016; Pan et al., 2017). Contrarily, humified pools are complex aromatic substances derived from decomposing lignocellulosic polymers (Stevenson, 1994; Vázquez et al., 2013) that can exhibit strong resistance against biodegradation (Marinari et al., 2010).

Several factors affect the quantity and quality of SOC and the water extractable DOM fraction in arable soils (Kalbitz et al., 2000). Besides soil temperature and water content (Burke et al., 2008), management practices (i.e. tillage, crop rotation) can influence SOC occurrence by (i) modifying soil physical structure and aggregation (Bongiovanni and Lobartini, 2006; Dieckow et al., 2009), (ii) changing the amount and quality of biomass-C inputs returned to the system (Chantigny, 2003;

* Corresponding authors.
E-mail addresses: carlos.romero89@outlook.com (C.M. Romero), rengel@montana.edu (R.E. Engel).

http://dx.doi.org/10.1016/j.geoderma.2017.06.029
Received 27 May 2017; Received in revised form 27 June 2017; Accepted 28 June 2017
0016-7061/ © 2017 Elsevier B.V. All rights reserved.

Table 1
Selected physical and chemical properties of soil at the experimental site.

Soil depth	Texture			BD[a]	CEC[b,g]	EC[c,h]	pH[i]	IC[d]	SOC[e,j]	TN[f,j]	C:N
	Sand	Silt	Clay								
cm	g kg^{-1}	g kg^{-1}	g kg^{-1}	g cm^{-3}	cmol$_c$ kg^{-1}	dS m^{-1}		g kg^{-1}	g kg^{-1}	g kg^{-1}	
0–10	173	613	214	1.16	18.41	0.11	6.28	0.58	13.0	1.3	9.7
10–20	163	606	231	1.34	17.97	0.07	6.59	0.87	9.6	1.1	8.7
20–30	158	630	212	1.43	19.42	0.05	7.22	1.64	7.7	0.9	8.5

[a] BD = bulk density.
[b] CEC = cation exchange capacity.
[c] EC = electrical conductivity.
[d] IC = inorganic carbon.
[e] SOC = soil organic carbon.
[f] TN = total nitrogen.
[g] Unbuffered 0.2 M NH_4Cl.
[h] 1:2 soil:water extract.
[i] 1:1 soil:water extract.
[j] LECO dry combustion (LECO Corp., St. Joseph, MI). Data taken from Engel et al. (2017).

Vázquez et al., 2016), and (iii) altering mineralization and humification pathways of plant residues in soil (Kalbitz et al., 2000; Vázquez et al., 2016). No-tillage (NT) management is often claimed to promote SOC accretion in surface soil (i.e. 0–30 cm) (Dieckow et al., 2009; Norton et al., 2012). However, the effect of long-term cropping intensity on SOC quality is not clear and still under debate; management practices may differentially affect SOC composition depending on site-specific environmental factors, such as climate and soil type (Embacher et al., 2007; Borisover et al., 2012).

In the northern Great Plains of North America, conversion from native semiarid shortgrass steppe to dryland wheat-fallow (W-F) cropping has resulted in severe soil erosion and a net loss of nutrients (DeLuca and Zabinski, 2011). A century of cultivation has decreased surface SOC and associated C fractions by ~50–60% (Norton et al., 2012; Hurisso et al., 2013). Recently, NT management has become increasingly popular, currently comprising 60% of dryland agriculture in this region (Hansen et al., 2012). With NT management, precipitation storage has improved and led to greater cropping system intensification with legume and/or oilseed crops being grown in rotation with wheat (Miller et al., 2015; Chen et al., 2015). More diverse and intensified NT systems have prompted SOC recovery through increased biomass-C inputs and minimal disturbance of soils. Several reports have documented higher SOC contents under NT annual cropping than conventional tillage (CT) with W-F systems (reviewed by Watts et al., 2011 and Collins et al., 2012). A recent study by Engel et al. (2017) quantified SOC levels among eight management systems in southern Montana, including CT fallow-wheat (F_{till}-W), NT spring pea/oilseed-wheat (P_g/O-W) and NT continuous wheat (W-W). After 10 yr, cumulative SOC stocks (0–30 cm) for NT W−W, NT P_g/O-W and F_{till}-W systems, average of two N levels, were equivalent to 38.4, 37.9, and 33.7 Mg C ha^{-1}, respectively. The degree to which SOC accumulated in soil was directly related to biomass-C inputs, particularly root and/or root-derived C. Engel et al. (2017) report SOC maintenance levels at 2.6 Mg ha^{-1} yr^{-1} of shoot + root + rhizodeposit C, or 7.0 Mg ha^{-1} yr^{-1} of net primary productivity (NPP), with accretion or loss occurring above or below these thresholds, respectively.

Accumulation of SOC after 10 yr of NT annual cropping (Engel et al., 2017) suggests recovery trends towards improved soil quality. Within this context, some differences in SOC composition were expected. The objective of this study was to characterize the chemistry of SOC following a continuum from minimally disturbed soils with high biomass-C inputs (i.e. NT annual cropping) to more strongly degraded fields (CT W-F). We extracted and further analyzed DOM from soil samples (0–30 cm) collected in 2012 along F_{till}-W, P_g/O-W and W-W fields (Engel et al., 2017) by combined use of non-destructive spectroscopic techniques such as UV/Vis absorbance and excitation emission matrix fluorescence spectroscopy (EEMs). We hypothesized that (i) additional biomass-C inputs under NT annual cropping (P_g/O-W, W-W) would increase plant-derived DOM constituents when compared to F_{till}-W, (ii) such changes would be associated with increasing SOC sequestration rates, and (iii) the influence of cropping systems on DOM properties is attenuated from surface soil to subsoil layers.

2. Materials and methods

2.1. Experimental site and study design

The soil analyzed in this study came from a long-term cropping system study established at Montana State University's Arthur H. Post Agronomy Research Farm, located 10 km west of Bozeman, Montana, USA (45° 40′ N, 111° 09′ W, elevation 1450 m). The location is characterized by a semiarid cold climate with annual precipitation of 411 mm and a mean annual temperature of 6.7 °C (Western Regional Climate Center, 2014). The soil is a Mollisol-type, classified as an Amsterdam silt loam (fine-silty, mixed, superactive, frigid Typic Haplustolls), generally deep and well-drained, and derived from loess-like deposits mixed with volcanic ash (Soil Survey Staff, 2013). Selected soil properties to a depth of 30 cm are presented in Table 1. The field study consisted of eight management systems replicated four times in a randomized complete block design, previously described by Engel et al. (2017). The water extractable DOM was characterized in three of the eight cropping systems, including F_{till}-W, P_g/O-W and W-W managed at a high N fertility level, and where large differences in SOC mass accretion were observed.

2.2. Soil sampling and processing

Soil sampling occurred in September 2012, or 10 yr after initiation of the field trial, using a truck mounted hydraulic probe. Triplicate soil cores (5 cm dia.) were collected to a depth of 30 cm from each plot, separated into three depth increments (0–10, 10–20, and 20–30 cm) and composited per depth. The composite core samples were placed in plastic-lined bags, dried (50 °C), and then crushed to pass through a 2-mm sieve. A subsample of the sieved material was then separated, and all identifiable crop residue material including roots were removed by hand-picking with tweezers prior to its analysis.

2.3. Dissolved organic matter

Soil (50 g) was added to an acid-washed (10% HCl), pre-combusted (425 °C, 4 h) 250-mL Erlenmeyer flask with 100 mL of ultrapure Milli-Q® water (≤ 18.2 MΩ cm^{-1}). The flasks were shaken (15 min,

100 rpm) and then allowed to settle for 15 min at room temperature (25 °C). The supernatant was subsequently passed through a pre-combusted Fisherbrand Glass Fiber Circle (Grade 6, 1.6 μm) and then vacuum filtered through a pre-combusted 0.7 μm Millipore glass fiber filter (EMD Millipore, Merk KGaA, Germany). Extracts were transferred to opaque, acid-washed, and pre-combusted glass bottles and stored in the dark at 4 °C prior to analysis within 24 h of sample extraction. Filtered Milli-Q® water blanks were collected in the same way as for the soil extracts. Water-extractable DOM concentration, expressed as dissolved organic carbon ([DOC]; mg C L^{-1}) and total nitrogen ([WEN]; mg N L^{-1}), was quantified in 15 mL aliquots using a total C and N Shimadzu combustion analyzer (TOC-V_{CSH}, Shimadzu Corp., Kyoto, Japan).

2.4. UV–Vis absorbance spectroscopy

Ultraviolet and visible light absorbance was measured in a 1 cm path-length quartz cuvette using a Genesys 10 Series spectrophotometer from 190 to 1100 nm (Thermo-Scientific, Rochester, NY) and VISIONlite software. Specific UV absorbance at 254 nm ($SUVA_{254}$, L mg^{-1} C m^{-1}), a proxy for DOM aromatic nature, was calculated as follows: $SUVA_{254} = 100 \times [Abs_{254} / (DOC)]$, where L is the optical path length (cm) and DOC is in mg C L^{-1} (Weishaar et al., 2003). Samples with absorbance values at 254 nm (Abs_{254}) > 0.3 a.u. (absorbance units) were diluted to volumes with Abs_{254} < 0.3 a.u. prior to collecting the entire absorbance and fluorescence spectra (Miller and McKnight, 2010). Dilution factors (2 and 4; diluted by half to a quarter the original concentrations) were subsequently used when post-processing the EEMs fluorescent data; UV/Vis absorbance values from 190 to 1100 nm were used to calculate necessary spectral corrections for primary and secondary inner filter effects (Tucker et al., 1992). Methodological and system blanks were run at the beginning of the experiment and between five sample sets.

2.5. Fluorescence spectroscopy

EEMs were obtained with a Horiba Jobin Yvon Fluoromax-4 spectrofluorometer (Horiba) equipped with a Xe lamp light source and 1 cm path-length quartz cuvette at 25 °C with the following specifications: excitation wavelengths of 240–450 nm scanned over 5 nm intervals, emission wavelengths of 300–560 nm recorded in 2 nm increments, data integration period 0.25 s, and 5 nm band pass for both excitation and emission monochromators. All data were generated in signal/reference mode to normalize the emission signal relative to the excitation light intensity. EEMs were normalized by the area under the Raman peak of a Milli-Q® water sample each day at Ex = 350 nm and Em = 365–450 nm. Post-collection data manipulation was performed to correct for inner filter effects, Raman scattering, and our method blank subtraction following the protocol outlined in D'Andrilli et al. (2017). System blanks of Milli-Q® water were scanned daily to monitor instrument performance, and also were used to post-process the EEMs of our methodological blanks to check for contamination.

DOM humification was measured from the EEMs data by calculating the humification index (HIX) (Zsolnay et al., 1999) for each sample. Briefly, the area in the upper quarter (434–480 nm; Em peak fluorescence intensities) was divided by the area in the lower quarter (300–344 nm) at Ex = 255 nm (Zsolnay et al., 1999). HIX is proportional to DOM condensation or humified state, and has been used to differentiate sources of DOM (i.e. fulvic acids vs. microbial biomass) upon soil drying (Zsolnay et al., 1999). The Fluorescence Index (FI) was calculated as the ratio of fluorescence emission intensity 470 nm and 520 nm (in Raman Units; R.U.), obtained at an excitation wavelength of 370 nm (Cory and McKnight, 2005). This index allows for discrimination between microbial (high FI ~1.8, bacteria leachate, algae) or terrestrially derived (low FI ~1.2, plant and soil) DOM (Cory and McKnight, 2005).

2.6. PARAFAC modelling – Multivariate analysis

Parallel factor (PARAFAC) analysis was applied to the EEMs data using drEEM (Decomposition Routines for Excitation Emission Matrices; v. 0.3.0) and the N-way toolbox in MATLAB R2016b (The MathWorks, Inc., Natick, MA) (Murphy et al., 2013; Stedmon and Bro, 2008). A non-negativity constraint was applied to both excitation and emission loadings, considering that negative fluorescent intensities and concentrations are chemically impossible (Ohno and Bro, 2006). No samples were identified as outliers, and PARAFAC analysis resolved four components comprising the 36 EEMs normalized data set, explaining 99.8% of the total variance. The PARAFAC model was validated by split-half analysis with all the components of the split model test finding a match with a Tucker correlation coefficient > 0.95 (Murphy et al., 2013). The Fluorescence Efficiency (FE, R.U. cm^{-1}), or quantum yield, was calculated by taking the ratio of PARAFAC component fluorescence maxima divided by the Abs_{254}, with higher FE indicating lower DOM size and/or molecular weight (Wu et al., 2003).

2.7. Linear statistical analyses

All statistical analyses were carried out using PROC GLM of SAS 9.4 (SAS Institute, Cary, NC). The effects of cropping system and soil depth on DOM size and spectroscopic features were analyzed with a two-way ANOVA. The assumptions of normal distribution and equal variance were tested using Shapiro–Wilk and Levene's tests, respectively. When significant effects were observed, treatment means were compared using Fisher's least significant difference (LSD) procedure at $\alpha = 0.05$. Single degree of freedom orthogonal contrasts were performed for the cropping system x soil depth interaction. Pearson correlation coefficients (*r*-value) were used to examine relationships between DOM properties. All figures were developed with SigmaPlot 13.0 software (Systat Software, San Jose, CA).

3. Results and discussion

3.1. Dissolved organic carbon concentration and C:N ratio

The distribution of DOC concentration, among each of the three soil depths and cropping systems, was summarized by box and whisker plots (Fig. 1). DOC concentration decreased with soil depth ($P < 0.0001$; Table 2). The 0–10 cm layer contained more DOC than the 10–20 and 20–30 cm layers, averaging 27.90, 14.23, and 12.85 mg C L^{-1}, respectively (Fig. 1). The contrast cropping system vs. soil depth showed larger DOC decreases under P_g/O-W and W-W than F_{till}-W (−50.05, −58.42% and −41.19%, respectively) ($P = 0.0178$; Table 2). DOC concentration was lowest in F_{till}-W, and highest in P_g/O-W or W−W, averaging 14.25, 19.31, and 21.42 mg C L^{-1}, respectively (Fig. 1). Furthermore, DOC concentration was strongly correlated to bulk SOC ($r = 0.81$, $P < 0.0001$) and TN levels (g kg^{-1}) ($r = 0.75$, $P < 0.0001$) reported by Engel et al. (2017) (Table 1).

The effect of cropping system on DOC concentration was consistent with the 10 yr change in C supply associated with NT annual cropping (Engel et al., 2017). Higher cumulative above- and below-ground C inputs (i.e. shoots, roots, and rhizodeposits) under P_g/O-W and W-W (29.1 and 30.7 Mg C ha^{-1}) when compared to F_{till}-W (21.1 Mg C ha^{-1}) increased SOC accretion and associated soil DOM fractions. This result was expected given the fact DOM is mostly replenished in solution by bulk SOC (Kalbitz et al., 2000; Akagi and Zsolnay, 2008). Soils at this field site (O'Dea et al., 2015) managed under F-W have poorer aggregate stability than NT annual cropping (101 and 192–220 g kg^{-1}), suggesting that physical protection likely prompted the accumulation of DOM in W-W or P_g/O-W fields.

The C:N ratio of DOM decreased with soil depth from 11.04 to 5.87 (Fig. 1). However, no significant differences were noted in DOM C:N ratio values among cropping systems ($P > 0.05$) (Table 2). The

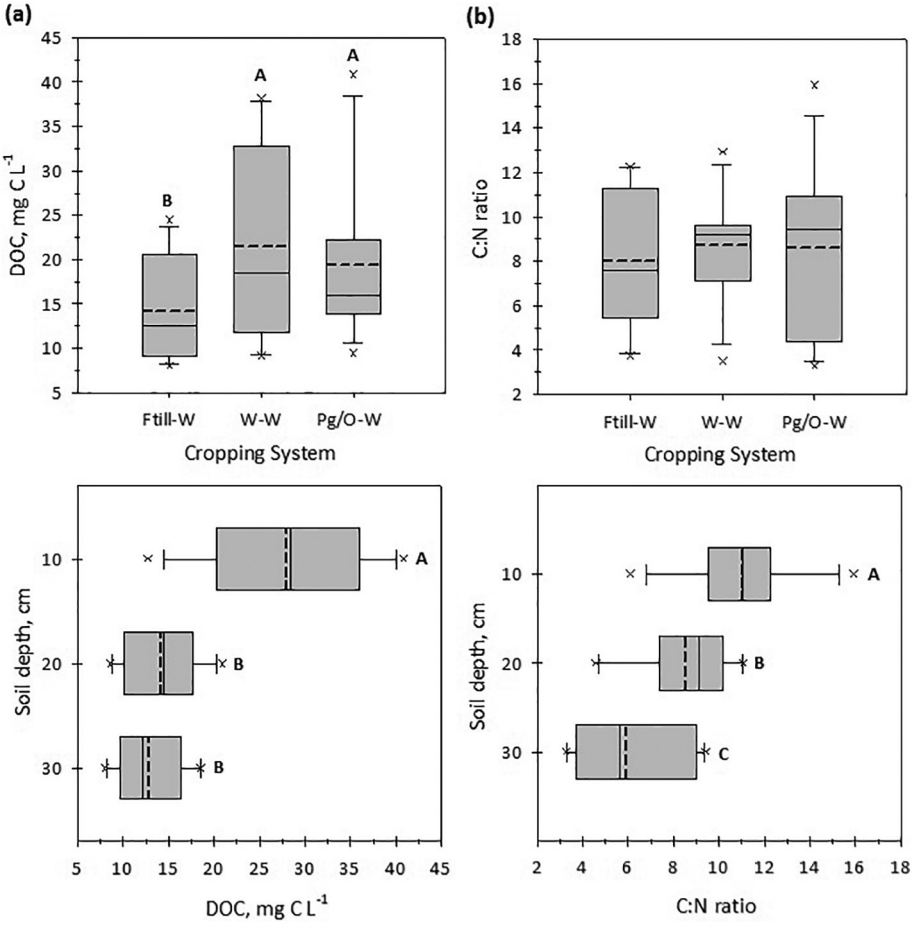

Fig. 1. Box and whisker plots of (a) dissolved organic carbon (DOC) concentration (mg C L^{-1}) and (b) C:N ratio from different cropping systems (F_{till}-W, conventional till fallow winter wheat; P_g/O-W no-till spring pea/oilseed-wheat; W-W no-till continuous wheat) and soil depths (0–10, 10–20 and 20–30 cm). Box plots show the 25 and 75 percentile ranges; solid and dashed inbox lines represent the median and mean, respectively; whiskers delimit the non-outlier ranges; and the symbol (x) represent outlier values. Different letters indicate significant differences (LSD Fisher test, $P < 0.05$).

observed higher C:N in the 0–10 cm layer clearly indicated an enrichment of N upon increasing soil depth (Toosi et al., 2012) regardless of the cropping system.

3.2. Optical characterization of DOM

3.2.1. Spectroscopic indices Abs_{254}, $SUVA_{254}$, HIX, FI, and FE

Estimates of Abs_{254} were significantly affected by soil depth and cropping system (Table 2). The Abs_{254} decreased from 0.55 to 0.10 with increasing soil depth (Fig. 2). This is consistent with results reported by Hassouna et al. (2012) and Toosi et al. (2012) and is mainly ascribed to adsorptive interactions of aromatic moieties with reactive mineral surfaces (Kaiser and Guggenberger, 2000), e.g. Ca^{2+}-bridging in neutral/alkaline soils (Oades, 1988). The Abs_{254} properties of DOM also changed with cropping system, and averaged 0.22, 0.31, and 0.35 for F_{till}-W, P_g/O-W, and W-W, respectively (Fig. 2). Higher inputs of plant biomass-C under NT annual cropping likely increased the concentration of lignin-like materials and/or other hydrophobic structures in soil (Capriel, 1997; Vázquez et al., 2016), further increasing DOM aromatic nature (Hassouna et al., 2012; Gao et al., 2017). The latter was substantiated by the modest ($r = 0.49$) but significant positive correlation ($P < 0.01$) between the Abs_{254} and the C:N ratio (Table 3). The overall depth pattern for $SUVA_{254}$ was similar to Abs_{254}; $SUVA_{254}$ decreased from 1.96 to 0.76 with increasing soil depth (Fig. 2). However, such trend was stronger under F_{till}-W than P_g/O-W and W-W (−55.77, −32.37% and −28.95%, respectively) ($P = 0.0121$; Table 2). Cropping system did not affect DOM $SUVA_{254}$ estimates ($P > 0.05$) (Table 2). Similarly, Abs_{254} yielded more pronounced relationships with other DOM properties than $SUVA_{254}$ (Table 3).

HIX increased significantly with soil depth from 2.22 to 2.93 (Fig. 2). This implied that DOM potentially contained old, highly processed structures within subsoil layers (Rumpel and Kogel-Knabner, 2011). Such a possibility is consistent with the modest, but significant negative correlation of the HIX and the C:N ratio ($r = -0.44$; $P < 0.01$) (Table 3). The content of N within soil organic matter is typically enriched by humification (Ewing et al., 2006). The

Table 2
Two-way ANOVA of the effect of cropping system and soil depth on dissolved organic carbon (DOC) concentration, C:N ratio, absorbance at 254 nm (Abs_{254}), specific UV absorbance at 254 nm ($SUVA_{254}$), humification index (HIX) and fluorescence index (FI) of DOM soil extracts.

Factors	df	DOC		C:N		Abs_{254}		$SUVA_{254}$		HIX		FI	
		F	*P*	*F*	*P*	*F*	*P*	*F*	*P*	*F*	*P*	*F*	*P*
Cropping system (CS)	2	6.70	0.0049	0.17	0.8439	4.14	0.0286	2.16	0.1369	3.91	0.0338	2.07	0.1484
Soil depth (D)	2	34.19	< 0.0001	11.87	0.0003	46.57	< 0.0001	57.63	< 0.0001	4.64	0.0197	1.82	0.1839
CS × D	4	2.37	0.0806	1.18	0.3476	0.70	0.6017	2.00	0.1274	0.19	0.9411	0.23	0.9217
0–10 vs. 10–30 × F_{till}-W vs. NT CS[a]	1	6.47	0.0178	0.52	0.4785	2.13	0.1579	7.38	0.0121	0.37	0.5482	0.44	0.5114

[a] F_{till}-W, conventional till fallow winter wheat; NT CS (P_g/O-W no-till spring pea/oilseed-wheat and W-W no-till continuous wheat).

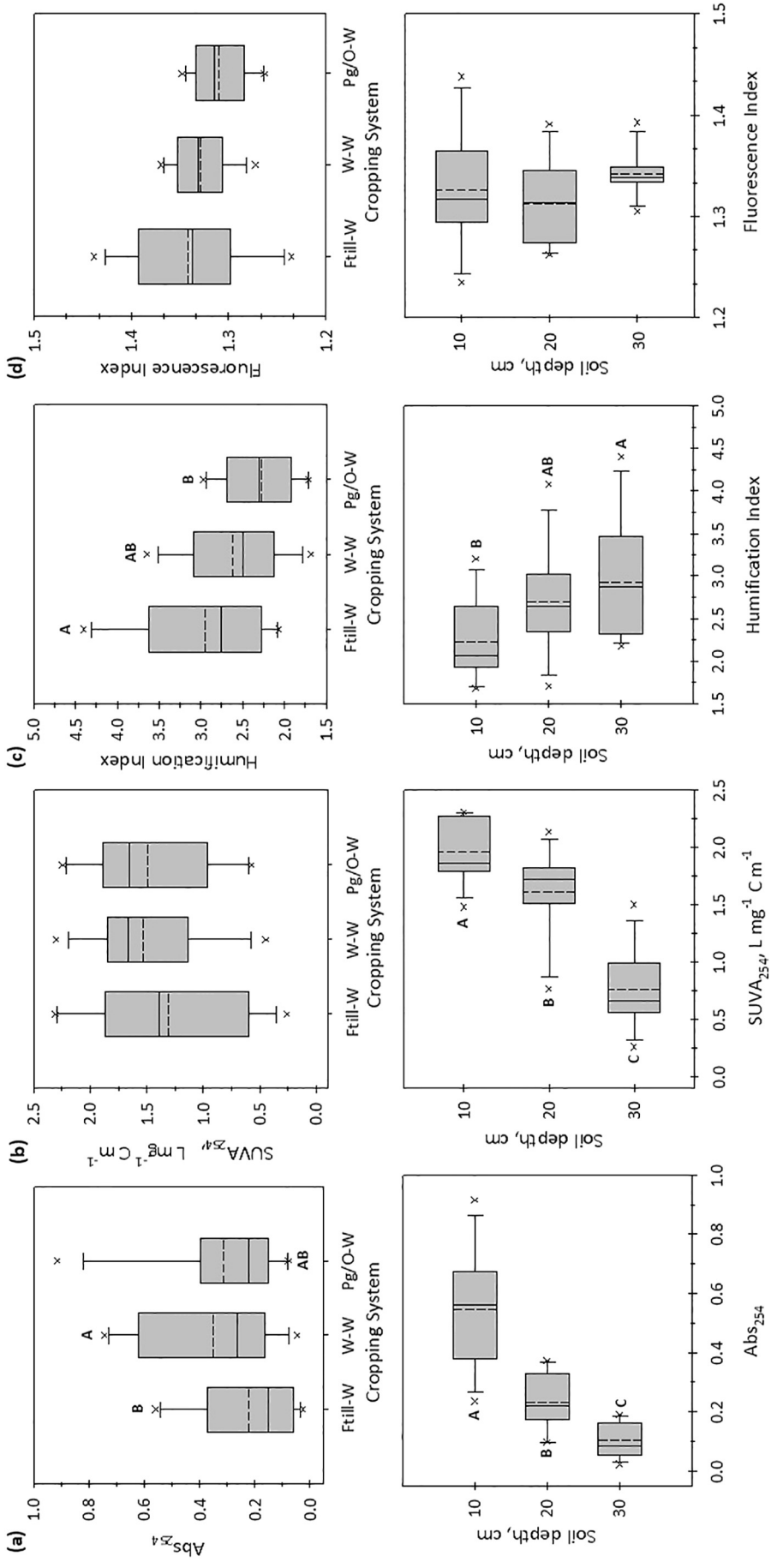

Fig. 2. Box and whisker plots of (a) absorbance at 254 nm (Abs_{254}), (b) specific UV absorbance at 254 nm ($SUVA_{254}$), (c) humification index and (d) fluorescence index from different cropping systems (F_{till}-W, conventional till fallow winter wheat; P_g/O-W no-till spring pea/oilseed-wheat; W-W no-till continuous wheat) and soil depths (0–10, 10–20 and 20–30 cm). Box plots show the 25 and 75 percentile ranges; solid and dashed inbox lines represent the median and mean, respectively; whiskers delimit the non-outlier ranges; and the symbol (x) represent outlier values. Different letters indicate significant differences (LSD Fisher test, $P < 0.05$).

Table 3
Pearson correlation coefficients (*r*) between various DOM parameters for all soil depths and cropping systems.

	DOC[a]	Abs_{254}	$SUVA_{254}$	HIX	FI	C:N	C1[b]	C2	C3	C4
Abs_{254}	0.94***	1.00								
$SUVA_{254}$	0.56***	0.77***	1.00							
HIX	− 0.52**	− 0.50**	− 0.42*	1.00						
FI	0.24	0.14	− 0.12	− 0.15	1.00					
C:N	0.42*	0.49**	0.55***	− 0.44**	0.05	1.00				
C1	0.92***	0.98***	0.74***	− 0.42**	0.24	0.44**	1.00			
C2	0.88***	0.97***	0.80***	− 0.41*	0.05	0.48**	0.97***	1.00		
C3	0.72***	0.75***	0.61***	− 0.81***	0.01	0.51**	0.70***	0.72***	1.00	
C4	0.90***	0.92***	0.63***	− 0.64***	0.21	0.50**	0.89***	0.85***	0.79***	1.00

[a] Dissolved organic carbon (DOC) concentration, absorbance at 254 nm (Abs_{254}), specific UV absorbance at 254 nm ($SUVA_{254}$), humification index (HIX), fluorescence index (FI), and C:N ratio of soil extracts.
[b] C1, C2, C3 and C4 refer to PARAFAC fluorescent components.
* Significant at $P < 0.05$.
** Significant at $P < 0.01$.
*** Significant at $P < 0.001$.

complexation of microbial biomass within mineral surfaces buffers N into more condensed, recalcitrant forms; narrowing soil C:N ratios (Ewing et al., 2006; Normand et al., 2017), yet increasing HIX (Martins et al., 2011). Across all depths, HIX varied from 2.95 in F_{till}-W to 2.28 in P_g/O-W soil (Fig. 2). The higher HIX under F_{till}-W suggested that DOM was depleted of more labile-C components. Highly disturbed arable soils have more humified SOC than NT (Milori et al., 2006; Martins et al., 2011) or grassland soils (Kalbitz et al., 1999). The physical breakdown of aggregates under CT fosters the microbial oxidation of native SOC and precludes the stabilization of fresh plant- and/or microbial-degradation byproducts (Ewing et al., 2006; Dieckow et al., 2009). The distribution of FI was not affected by cropping system or soil depth (Table 2), and oscillated between 1.23 and 1.44 (Fig. 2); lower than the estimated average for arable soils (i.e. 1.50–1.90) (Hassouna et al., 2012; Sun et al., 2017). Terrestrial, plant-derived material dominated DOM fluorescence (Cory and McKnight, 2005); our sampling scheme was perhaps not deep enough to catch microbial, autochthonous signatures of DOM occurring in subsoil layers (Hassouna et al., 2012). FE increased sharply with soil depth and was generally higher under F_{till}-W than P_g/O-W or W-W (Table S1). This indicated DOM was comprised by low molecular size constituents within subsoil layers, regardless of its intrinsic chemical character (Wu et al., 2003). Reduced biomass-C inputs under F_{till}-W relative to P_g/O-W or W-W likely prompted soil microorganisms to further process the already existing pool of SOC (González-Pérez et al., 2007); particularly when considering a microbial community shift towards simple, energy-poor DOM (Nunan et al., 2015).

Humification is typically associated with aromaticity and the polycondensed status of organic structures in SOC (Stevenson, 1994); several reports show high correlations between humification and aromatic humic substances in soil (Fuentes et al., 2006; Marinari et al., 2010). However, an opposite trend was observed in our study among Abs_{254}, $SUVA_{254}$ and HIX (Table 3). DOM composition was more humified and less aromatic as a function of soil depth. Our results are in agreement with findings by Sanderman et al. (2008) and Hassouna et al. (2012) in grassland and arable soils, and indicate a shift from fresh plant-derived to older, highly decomposed DOM upon increasing soil depth.

3.2.2. EEMs and PARAFAC components of DOM

Average EEMs, representative of cropping system by soil depth fluorescent profiles, are shown in Fig. S1. All samples contained DOM species fluorescing at low (< 240–280/300–330 nm) and high (< 240–275/390–540 nm) excitation/emission (Ex/Em) wavelengths, including fluorescence maxima overlapping EEM regions commonly associated with fluorophore peaks B (tyrosine-like), T (tryptophan-like), A (humic-like), and C (humic-like) (Coble, 1996; Coble et al., 1998). Fluorescence intensities decreased upon increasing soil depth and NT annual cropping (i.e. P_g/O-W and W-W) contained higher fluorescence intensities than F_{till}-W soils (Fig. S1). Since DOM is a complex mixture of biomolecules that can fluoresce in overlapping Ex/Em wavelength regions, the application of PARAFAC analysis was used to resolve the EEMs into individual DOM fluorescing components characterized by their Ex/Em maxima (Coble et al., 2014; D'Andrilli et al., 2017).

Four different fluorescent components, hereafter referred to as components one through four (C1-C4), were identified by PAFAFAC analysis (contour plots Fig. 3a; loading scores Fig. S2). The spectral Ex/Em maxima of these components and descriptions of similar DOM markers reported in the literature are summarized in Table 4. PARAFAC C1 and C2 resembled mid- and large-size humic-like fluorophores characteristic of soil, sediment, and freshwater environments (Ishii and Boyer, 2012). Fluorescent markers in this region are linked with recalcitrant plant or soil-derived constituents highly resistant to microbial decomposition (Cory and McKnight, 2005), but susceptible to photochemical and abiotic degradation (Coble et al., 2014).

PARAFAC C3 showed maximum fluorescence in a region analogous to the secondary fluorescence of B-peak (Ex/Em: 230/305 nm); a region commonly ascribed to microbial-derived DOM, but also more recently attributed to simple phenolic compounds (i.e. monolignols) of plant origin (Coble et al., 2014). PARAFAC C3 also contained fluorescence indicative of more complex lignin-like precursors, e.g. Ex 240 nm spanning Em 308–556 nm. Thus, we attribute C3 fluorescence to include simple and somewhat more complex lignin-like chemical species. PARAFAC C4 exhibited maximum fluorescence in a region analogous to the primary fluorescence of B-peak and secondary fluorescence of T-peak (Ex/Em 275/305–340 nm) (Coble, 1996; Coble et al., 1998); overlapping fluorescence between protein- and tannin-like DOM markers (Cuss and Gueguen, 2013; Coble et al., 2014).

In terrestrial ecosystems, DOM exists as a mixture of organic fragments at various stages of oxidation and decay (Masoom et al., 2016). Microbial processing of vegetative inputs alters DOM reactivity by increasing soil aggregation and adsorptive processes within mineral surfaces (Lehmann and Kleber, 2015). Unfortunately, we cannot determine the absolute soil versus plant origin of DOM by fluorescence spectroscopy, thus can only consider C1, C2, C3 and C4 to be a mixture of terrestrially-derived signatures with minimal biological contribution (i.e. FI: 1.23–1.44). Nevertheless, our PARAFAC model identified chemical species at different stages of decomposition. Average FE ($n = 36$) was higher for C1 (1.92 ± 0.25) followed by C3 (1.77 ± 0.26), C2 (1.19 ± 0.16), and C4 (0.67 ± 0.08), indicating molecular weights decreased in the order C4 > C2 > C3 > C1. Taken together, we infer fluorescent DOM chemical character is best described when considering the progressive transformation of plant and microbial-derived biopolymers in solution. Future research should incorporate a DOM

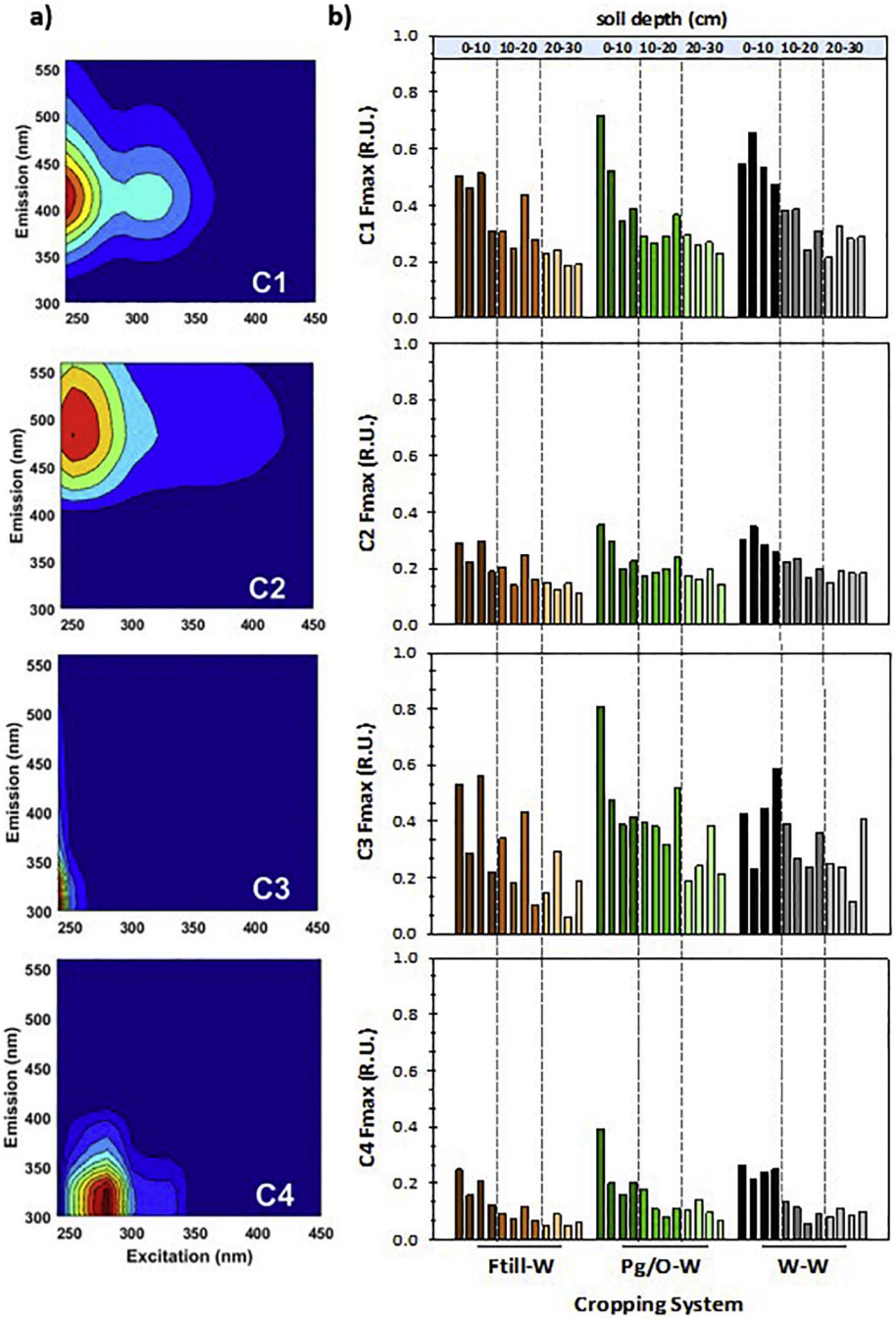

Fig. 3. PARAFAC analysis results of soil DOM showing a) components one through four (C1, C2, C3, and C4) and b) fluorescence maxima (Fmax) in Raman units (R.U.) of each component (n = 36) from different cropping systems (F_{till}-W, conventional till fallow winter wheat; P_g/O-W no-till spring pea/oilseed-wheat; W-W no-till continuous wheat) and soil depths (0–10, 10–20 and 20–30 cm).

continuum model (Lehmann and Kleber, 2015), rather than classifying fluorescent components as only humic- and/or protein-like chemical species.

3.2.3. Variations of PARAFAC components

The distributions of PARAFAC component Ex/Em fluorescent maxima (Fmax; R.U.) among soil depths and cropping systems are presented in Fig. 3b. The Fmax was assumed to be a proxy for the relative concentration of each PARAFAC component in each sample (Murphy et al., 2013). In general, Fmax decreased with soil depth (Fig. 3b; Fig. 4), with a further significant decrease in Fmax below the 10–20 cm depth only detected for C2 (Table 5). As already discussed, adsorption processes within the soil matrix can gradually affect the vertical occurrence of DOM fractions (Kaiser and Guggenberger, 2000). Alternatively, microbial degradation of labile-C, occurring in surface soil, can also limit the downward movement of DOM (Marinari et al., 2010).

Across all depths, mean Fmax of C1 and C3 were similar among F_{till}-W, P_g/O-W and W-W (Table 5). However, significant increases in average Fmax were reported for NT annual cropping (P_g/O-W and W−W) for both C2 (P = 0.0422) and C4 (P = 0.0171) over F_{till}-W (Table 5). No significant variation in Fmax was determined for each component when comparing P_g/O-W and W-W cropping systems. Accordingly, NT annual cropping increased Fmax of PARAFAC components, whereas F_{till}-W led to a more depleted fluorescent DOM pool. This suggested DOM composition to be mainly driven by the amount of biomass-C inputs rather than the quality of crop residues returned to the system. Moreover, cumulative changes in DOM chemical character influenced bulk SOC dynamics. The occurrence of PARAFAC components at high Ex/Em wavelengths (C1 and C2) reflected reasonably well with the ΔSOC gradient imposed by F_{till}-W, P_g/O-W, and W-W (Fig. 5), which averaged − 3.80, 1.51 and 2.70 Mg C ha^{-1}, respectively (Engel

Table 4
Approximate location of peaks [excitation and emission ($\lambda_{ex}/\lambda_{em}$, nm)] of PARAFAC identified components for DOM soil extracts.

Component no.	Current study ($\lambda_{ex}/\lambda_{em}$, nm)	Previous models ($\lambda_{ex}/\lambda_{em}$, nm)	Literature component description	Previous PARAFAC assignment	Current study component description
C1	< 240–250/390–440	< 240–260/374–450[a] 240/405–408[b] < 250/410[c] < 250/397[h]	Terrestrial and marine humic-like	C3[a],C2[b],C2[c],C2[h]	Terrestrial humic-like (plant/soil derived)
C2	< 240–275/455–540	< 240–275/434–520[a] 240/474–480[b] 260/500[c] 260/490[d] > 240/465[f] < 250/460[h]	Terrestrial humic-like	C2[a],C1[b],C4[c],C3[d], C2[f],C1[h]	Terrestrial humic-like (plant/soil derived)
C3	< 240/303–312	240/312–315[b] 273/309[f] < 230–300[i] 220/320[j]	Tyrosine-like	C3[b],C5[f], C5[i],C3[j]	Monolignol-like (lignin precursor)
C4	280/300–330	280/328[d] 260/340[e] 270/354[f] 285/354[g] 260/320[h]	Tryptophan-like; phenol-like	C6[d],C2[e],C4[f],C3[g],C4[h]	Protein-like; tannin-like

[a] Ishii and Boyer (2012).
[b] Zhao et al. (2012).
[c] Sharma et al. (2017).
[d] Murphy et al. (2008).
[e] Pan et al. (2017).
[f] Ohno and Bro (2006).
[g] Borisover et al. (2012).
[h] Cao et al. (2016).
[i] Zhou et al. (2017).
[j] Gao et al. (2017).

et al., 2017). The higher SOC accretion rate by W-W vs. P_g/O-W likely resulted from slightly greater biomass-C inputs under W-W than P_g/O-W and lower quality (high C:N ratio) of W—W residues (O'Dea et al., 2015; Duval et al., 2016). This response was consistent with reports by Kaiser and Guggenberger (2000) and Kramer et al. (2012) that recalcitrant, aromatic DOM is the greatest contributor for long-term SOC storage.

Strong positive correlations were found between all four PARAFAC components, Abs_{254}, and DOC concentrations (Table 3). Both UV-absorbing compounds and fluorescent molecules contributed to the bulk pool of DOM concentration (Borisover et al., 2012; Sharma et al., 2017). Fmax values increased strongly with higher SOC concentrations (Fig. 4). The depth pattern was similar among PARAFAC components; Fmax was higher in surface soil, particularly under NT annual cropping (P_g-O/W, W-W). It is important to note, however, the trend was more pronounced within C1 and C3, than C2 or C4 (Fig. 4), describing highly condensed DOM with lower molecular weights and aromaticity at depth.

4. Conclusions

The results of this study supported our hypothesis that changes in SOC accretion patterns altered the chemical structure of SOC. Characterization of soil water extractable DOM revealed contrasting structural features after 10 yr of cropping intensity and tillage (Engel et al., 2017). Annual cropping with NT management increased the DOM pool concentration and compositional diversity; higher inputs of biomass-C promoted the accumulation of fresh, plant-derived DOM constituents in solution relative to the conventional F_{till}-W management. Contrarily, DOM extracted from F_{till}-W was more humified than P_g/O-W or W-W, which may reflect the more decomposed, recalcitrant native SOC pool. DOM composition surveyed by EEMs can be used to track SOC quality changes and provide further insights on the mechanisms driving SOC microbial processing, decomposition, and sequestration. Accretion of SOC was accompanied by the presence of a larger and more enriched DOM pool, likely favoring the uptake of nutrients by winter wheat.

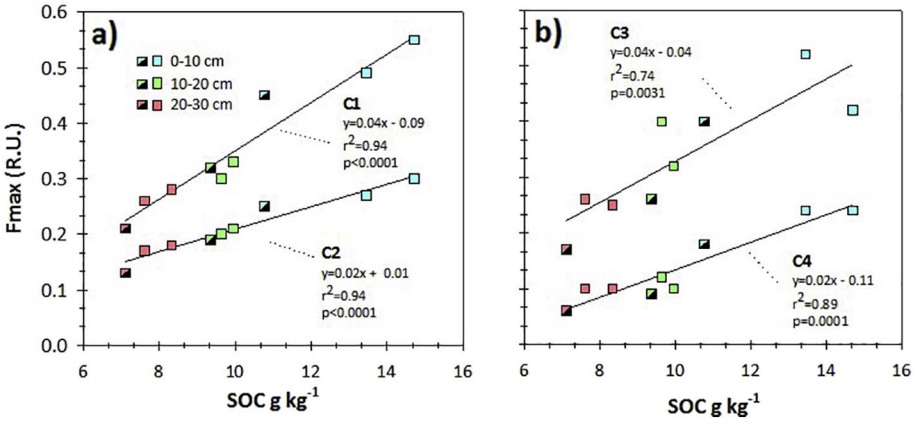

Fig. 4. Relationship between average fluorescence maxima (Fmax) in Raman units (R.U.) of a) high- (C1, C2) and b) low- (C3, C4) Ex/Em PARAFAC components and soil organic carbon (SOC) concentration (g kg^{-1}) from different soil depths (0–10, 10–20 and 20–30 cm). Filled and semi-filled squares represent annual cropping (P_g/O-W and W-W) and F_{till}-W, respectively.

Table 5
Two-way ANOVA of the effect of cropping system (F_{till}-W, conventional till fallow winter wheat; P_g/O-W no-till spring pea/oilseed-wheat; W-W no-till continuous wheat) and soil depth (0–10, 10–20 and 20–30 cm) on fluorescence maxima (Fmax) in Raman units (R.U.) of PARAFAC components one through four (C1, C2, C3 and C4).

		PARAFAC components							
		C1		C2		C3		C4	
		Fmax (R.U.)							
Cropping system (CS)									
F_{till}-W		0.32 ± 0.04		0.19 ± 0.02		0.28 ± 0.05		0.11 ± 0.02	
P_g/O-W		0.35 ± 0.04		0.21 ± 0.02		0.39 ± 0.05		0.15 ± 0.03	
W-W		0.39 ± 0.04		0.23 ± 0.02		0.33 ± 0.04		0.15 ± 0.02	
Soil depth (D)									
0–10 cm		0.50 ± 0.03[a]		0.27 ± 0.02[a]		0.45 ± 0.05[a]		0.22 ± 0.02[a]	
10–20 cm		0.32 ± 0.02[b]		0.20 ± 0.01[b]		0.33 ± 0.03[b]		0.10 ± 0.01[b]	
20–30 cm		0.25 ± 0.01[b]		0.16 ± 0.01[c]		0.23 ± 0.03[b]		0.09 ± 0.01[b]	
		ANOVA							
Factor	df	C1		C2		C3		C4	
		F	*P*	*F*	*P*	*F*	*P*	*F*	*P*
CS	2	1.77	0.1927	2.56	0.0980	2.27	0.1251	3.38	0.0510
F_{till}-W vs. NT CS[d]	1	2.45	0.1305	4.60	0.0422	3.15	0.0886	6.56	0.0171
P_g/O-W vs. W-W	1	1.08	0.3092	0.52	0.4769	1.39	0.2504	0.19	0.6647
D	2	30.06	< 0.0001	25.67	< 0.0001	8.30	0.0018	37.39	< 0.0001
CS × D	4	0.43	0.7850	0.19	0.9431	0.16	0.9580	0.29	0.8805

Data are mean ± SE (n = 12). Means followed by a common letter within a column are not significantly different (LSD Fisher $P < 0.05$).
[d] NT CS, no-till P_g/O-W and W-W.

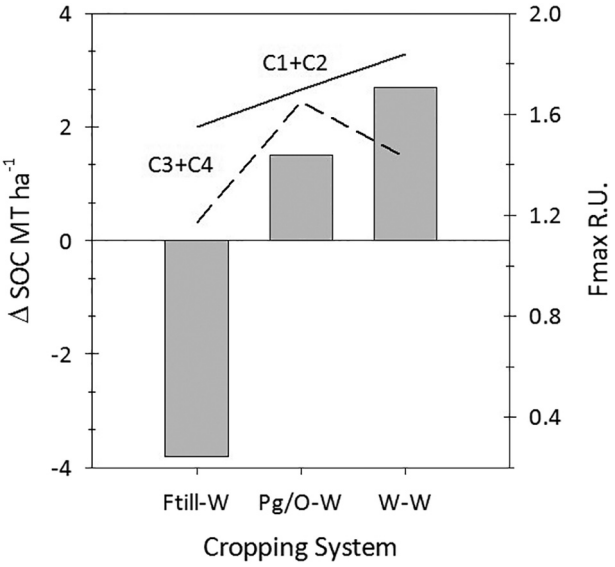

Fig. 5. Cumulative fluorescence maxima (Fmax) in Raman units (R.U.) of humic-like (C1 and C2), monolignol-like (C3) and protein/tannin-like (C4) PARAFAC components among cropping systems (F_{till}-W, conventional till fallow winter wheat; P_g/O-W no-till spring pea/oilseed-wheat; W-W no-till continuous wheat) with different 10 yr soil organic carbon (SOC) accrual patterns (ΔMT ha^{-1}) in the 0–30 cm layer. Data adapted from Engel et al. (2017).

Supplementary data to this article can be found online at http://dx.doi.org/10.1016/j.geoderma.2017.06.029.

Acknowledgements

This work was supported by USDA-NIFA project #MONB00346 “Nutrient cycling and management in Montana's agricultural soils” granted to Dr. Richard E. Engel. We thank Dr. Christine M. Foreman for use of laboratory instrumentation at Montana State University to conduct the bulk optical spectroscopic DOM analyses. In addition, we acknowledge two anonymous reviewers for providing helpful comments and constructive inputs that improved the manuscript.

References

Akagi, J., Zsolnay, Á., 2008. Effects of long-term de-vegetation on the quantity and quality of water extractable organic matter (WEOM): biogeochemical implications. Chemosphere 72, 1462–1466.
Bolan, N.S., Adriano, D.C., Kunhikrishnan, A., James, T., McDowell, R., Senesi, N., 2011. Dissolved organic matter: biogeochemistry, dynamics and environmental significance in soils. Adv. Agron. 110, 1–75.
Bongiovanni, M.D., Lobartini, J.C., 2006. Particulate organic matter, carbohydrate, humic acid contents in soil macro- and microaggregates as affected by cultivation. Geoderma 136, 660–665.
Borisover, M., Lordian, A., Levy, G.J., 2012. Water-extractable soil organic matter characterization by chromophoric indicators: effects of soil type and irrigation water quality. Geoderma 179-180, 28–37.
Burke, I.C., Mosier, A.R., Hook, P.B., Milchunas, D.G., et al., 2008. Soil organic matter and nutrient dynamics of shortgrass steppe ecosystems. In: Lauenroth, W.K., Burke, I.C. (Eds.), Ecology of the Shortgrass Steppe. Oxford University Press, New York, pp. 306–341.
Cao, F., Medeiros, P.M., Miller, W.L., 2016. Optical characterization of dissolved organic matter in the Amazon River plume and the Adjacent Ocean: examining the relative role of mixing, photochemistry, and microbial alterations. Mar. Chem. 186, 178–188.
Capriel, P., 1997. Hydrophobicity of organic matter in arable soils: influence of management. Eur. J. Soil Sci. 48, 457–462.
Chantigny, M.H., 2003. Dissolved and water-extractable organic matter in soils: a review on the influence of land use and management practices. Geoderma 113, 357–380.
Chen, C., Bekkerman, A., Afshar, R.K., Neill, K., 2015. Intensification of dryland cropping systems for bio-feedstock production: evaluation of agronomic and economic benefits of *Camelina sativa*. Ind. Crop. Prod. 71, 114–121.
Coble, P.G., 1996. Characterization of marine and terrestrial DOM in seawater using excitation-emission matrix spectroscopy. Mar. Chem. 51, 325–346.
Coble, P.G., Del Castillo, C.E., Avril, B., 1998. Distribution and optical properties of CDOM in the Arabian Sea during the 1995 Southwest Monsoon. Deep-Sea Res. II 45, 2195–2223.
Coble, P.G., Lead, J., Baker, A., Reynolds, D.M., Spencer, R.G.M., 2014. Aquatic Organic Matter Fluorescence. Cambridge University Press, New York, NY, pp. 35–74.
Collins, H.P., Mikha, M.M., Brown, T.T., Smith, J.L., Huggins, D., Sainju, U.M., 2012. Agricultural management and soil carbon dynamics: Western U.S. Croplands. In: Liebig, M.K., Franzluebbers, A.J., Follet, R.F. (Eds.), Managing Agricultural Greenhouse Gases. Elsevier, Amsterdam, The Netherlands, pp. 59–77.
Cory, R.M., McKnight, D.M., 2005. Fluorescence spectroscopy reveals ubiquitous presence of oxidized and reduced quinones in dissolved organic matter. Environ. Sci. Technol. 39, 8142–8149.
Cuss, C.W., Gueguen, C., 2013. Distinguishing dissolved organic matter at its origin: size and optical properties of leaf-litter leachates. Chemosphere 92, 1483–1489.
D'Andrilli, J., Foreman, C.M., Sigl, M., Priscu, J.C., McConnell, J.R., 2017. A 21,000 year record of fluorescent organic matter markers in the WAIS Divide ice core. Clim. Past 13, 533–544.
DeLuca, T.H., Zabinski, C.A., 2011. Prairie ecosystems and the carbon problem. Front. Ecol. Environ. 9, 407–413.
Dieckow, J., Bayer, C., Conceicao, P.C., Zanatta, J.A., Martin-Neto, L., Milori, D.B.M., Salton, J.C., Macedo, M.M., Mielniczuk, J., Hernani, L.C., 2009. Land use, tillage, texture and organic matter stock and composition in tropical and subtropical Brazilian soils. Eur. J. Soil Sci. 60, 240–249.

Duval, M.E., Galantini, J.A., Capurro, J.E., Martinez, J.M., 2016. Winter cover crops in soybean monoculture: effects on soil organic carbon and its fractions. Soil Tillage Res. 161, 95–105.
Embacher, A., Zsolnay, A., Gattinger, A., Munch, J.C., 2007. The dynamics of water extractable organic matter (WEOM) in common arable topsoils: I. Quantity, quality and function over a three year period. Geoderma 139, 11–22.
Engel, R.E., Miller, P.R., McConkey, B.G., Wallander, R., 2017. Soil organic carbon changes to increasing cropping intensity and no-till in a semiarid climate. Soil Sci. Soc. Am. J. 81, 404–413.
Ewing, S.A., Sanderman, J., Baisden, W.T., Wang, Y., Amundson, R., 2006. Role of large-scale soil structure in organic carbon turnover: evidence from California grassland soils. J. Geophys. Res. Biogeosci. 111, G03012.
Fuentes, M., González-Gaitano, G., García-Mina, J.M., 2006. The usefulness of UV–visible and fluorescence spectroscopies to study the chemical nature of humic substances from soils and composts. Org. Geochem. 37, 1949–1959.
Gao, J., Liang, C., Shen, G., Lv, J., Wu, H., 2017. Spectral characteristics of dissolved organic matter in various agricultural soils throughout China. Chemosphere 176, 108–116.
González-Pérez, M., Milori, D.M.B.P., Colnago, L.A., Martin-Neto, L., Melo, W.J., 2007. A laser-induced fluorescence spectroscopic study of organic matter in a Brazilian Oxisol under different tillage system. Geoderma 138, 20–24.
Hansen, N.C., Allen, B.L., Baumhardt, R.L., Lyon, D.J., 2012. Research achievements and adoption of no-till, dryland cropping in the semi-arid US Great Plains. Field Crop Res. 132, 196–203.
Hassouna, M., Théraulaz, F., Massiani, C., 2012. Production and elimination of water extractable organic matter in a calcareous soil as assessed by UV/Vis absorption and fluorescence spectroscopy of its fractions isolated on XAD-8/4 resins. Geoderma 189-190, 404–414.
Hurisso, T.T., Norton, J.B., Norton, U., 2013. Soil profile carbon and nitrogen in prairie, perennial grass–legume mixture and wheat–fallow production in the central High Plains, USA. Agric. Ecosyst. Environ. 181, 179–187.
Ishii, S.K.L., Boyer, T.H., 2012. Behaviour of reoccurring PARAFAC components in fluorescent dissolved organic matter in natural and engineered systems: a critical review. Environ. Sci. Technol. 46, 2006–2017.
Kaiser, K., Guggenberger, G., 2000. The role of DOM sorption to mineral surfaces in the preservation of organic matter in soils. Org. Geochem. 31, 711–725.
Kalbitz, K., Geyer, W., Geyer, S., 1999. Spectroscopic properties of dissolved humic substances – a reflection of land use history in a fen area. Biogeochemistry 47, 219–238.
Kalbitz, K., Solinger, S., Park, J.H., Michalzik, B., Matzner, E., 2000. Controls on the dynamics of dissolved organic matter in soils: a review. Soil Sci. 165, 277–304.
Kramer, M.G., Sanderman, J., Chadwick, O.A., Chorover, J., Vitousek, P.M., 2012. Long-term carbon storage through retention of dissolved aromatic acids by reactive particles in soil. Glob. Chang. Biol. 18, 2594–2605.
Lehmann, J., Kleber, M., 2015. The contentious nature of soil organic matter. Nature 528, 60–68.
Marinari, S., Dell'Abate, M.T., Brunetti, G., Dazzi, C., 2010. Differences of stabilized organic carbon fractions and microbiological activity along Mediterranean Vertisols and Alfisols profiles. Geoderma 156, 379–388.
Martins, T., Saab, S.C., Milori, D.M.B.P., Brinatti, A.M., Rosa, J.A., Cassaro, F.A.M., Pires, L.F., 2011. Soil organic matter humification under different tillage managements evaluated by laser induced fluorescence (LIF) and C/N ratio. Soil Tillage Res. 111, 231–235.
Masoom, H., Courtier-Murias, D., Farooq, H., Soong, R., Kelleher, B.P., Zhang, C., Maas, W.E., Fey, M., Kumar, R., Monette, M., Stronks, H.J., Simpson, M.J., Simpson, A.J., 2016. Soil organic matter in its native state. Unravelling the most complex biomaterial on earth. Environ. Sci. Technol. 50, 1670–1680.
Miller, M.P., McKnight, D.M., 2010. Comparison of seasonal changes in fluorescent dissolved organic matter among aquatic lake and stream sites in the Green Lakes Valley. J. Geophys. Res. Biogeosci. 115.
Miller, P.R., Bekkerman, A., Jones, C.A., Burgess, M.H., Holmes, J.A., Engel, R.E., 2015. Pea in rotation with wheat reduced uncertainty of economic returns in southwest Montana. Agron. J. 107, 541–550.
Milori, D.M.B.P., Galeti, H.V.A., Martin-Neto, L., Dieckow, J., González-Pérez, M., Bayer, C., Salton, J., 2006. Organic matter study of whole soil samples using laser-induced fluorescence spectroscopy. Soil Sci. Soc. Am. J. 70, 57–63.
Murphy, K.R., Stedmon, C.A., Waite, T.D., Ruiz, G.M., 2008. Distinguishing between terrestrial and autochthonous organic matter sources in marine environments using fluorescence spectroscopy. Mar. Chem. 108, 40–58.
Murphy, K.R., Stedmon, C.A., Graeber, D., Bro, R., 2013. Fluorescence spectroscopy and multi-way techniques. PARAFAC. Anal. Methods 5, 6557–6566.
Normand, A.E., Smith, A.N., Clark, M.W., Long, J.R., Reddy, K.R., 2017. Chemical composition of soil organic matter in a subarctic peatland: influence of shifting vegetation communities. Soil Sci. Soc. Am. J. 81, 41–49.
Norton, J.B., Mukhwana, E.J., Norton, U., 2012. Loss and recovery of soil organic carbon and nitrogen in a semiarid agroecosystem. Soil Sci. Soc. Am. J. 76, 505–514.
Nunan, L., Lerch, T.Z., Pouteau, V., Mora, P., Changey, F., Katterer, T., Giusti-Miller, S., Herrmann, A.M., 2015. Metabolising old soil carbon: simply a matter of simply organic matter? Soil Biol. Biochem. 88, 128–136.
Oades, J.M., 1988. The retention of organic matter in soils. Biogeochemistry 5, 35–70.
O'Dea, J.K., Jones, C.A., Zabinski, C.A., Miller, P.R., Keren, I.N., 2015. Legume, cropping intensity, and N-fertilization effects on soil attributes and processes from an eight-year-old semiarid wheat system. Nutr. Cycl. Agroecosyst. 102, 179–194.
Ohno, T., Bro, R., 2006. Dissolved organic matter characterization using multiway spectral decomposition of fluorescence landscapes. Soil Sci. Soc. Am. J. 70, 2028–2037.
Pan, H., Yu, H., Song, Y., Liu, R., Du, E., 2017. Application of solid surface fluorescence EEM spectroscopy for tracking organic matter quality of native halophyte and furrow-irrigated soils. Ecol. Indic. 73, 88–95.
Rumpel, C., Kogel-Knabner, I., 2011. Deep soil organic matter-a key, but poorly understood component of terrestrial C cycle. Plant Soil 338, 143–158.
Sanderman, J., Baldock, J.A., Amundson, R., 2008. Dissolved organic carbon chemistry and dynamics in contrasting forest and grassland soils. Biogeochemistry 89, 181–198.
Sharma, P., Laor, Y., Raviv, M., Medina, S., Saadi, I., Krasnovsky, A., Vager, M., Levy, G.J., Bar-Tal, A., Borisover, M., 2017. Compositional characteristics of organic matter and its water-extractable components across a profile of organically managed soil. Geoderma 286, 73–82.
Soil Survey Staff, 2013. Web soil survey. NRCS, USDA. http://websoilsurvey.nrcs.usda.gov (accessed 16/2/2017).
Stedmon, C.A., Bro, R., 2008. Characterizing dissolved organic matter fluorescence with parallel factor analysis: a tutorial. Limnol. Oceanogr. Methods 6, 572–579.
Stevenson, F.J., 1994. Humus Chemistry. Genesis, Composition, Reactions. John Wiley and Sons, New York, NY.
Sun, H.Y., Koal, P., Gerl, G., Schroll, R., Joergensen, R.G., Munch, J.C., 2017. Response of water extractable organic matter and its fluorescence fractions to organic farming and tree species in poplar and *Robinia*-based alley cropping agroforestry systems. Geoderma 290, 83–90.
Toosi, E.R., Castellano, M.J., Singer, J.W., Mitchell, D.C., 2012. Differences in soluble organic matter after 23 years of contrasting soil management. Soil Sci. Soc. Am. J. 76, 628–637.
Tucker, S.A., Amszi, V.L., Acree, W.E., 1992. Primary and secondary inner filtering - effect of $K_2Cr_2O_7$ on fluorescence emission intensities of quinine sulfate. J. Chem. Educ. 69, A8–A12.
Vázquez, C., Merlo, C., Noé, L., Romero, C., Abril, A., Carranza, C., 2013. Sustainability/resilience of soil organic matter components in an Argentinean arid region. Spanish J. Soil Sci. 3, 73–77.
Vázquez, C., Iriarte, A.G., Merlo, C., Abril, A., Kowaljow, E., Meriles, J.M., 2016. Land use impact on chemical and spectroscopical characteristics of soil organic matter in an arid ecosystem. Environ. Earth Sci. 75, 883.
Watts, J.D., Lawrence, R.L., Miller, P., Montagne, C., 2011. An analysis of cropland carbon sequestration estimates for North Central Montana. Clim. Chang. 108, 301–331.
Weishaar, J.L., Aiken, G.R., Bergamaschi, B.A., Fram, M.S., Fujii, R., Mopper, K., 2003. Evaluation of specific ultraviolet absorbance as an indicator of the chemical composition and reactivity of dissolved organic carbon. Environ. Sci. Technol. 37, 4702–4708.
Western Regional Climate Center, 2014. Bozeman 6 W exp. farm, Montana, 1981–2010 temperature and precipitation. http://www.wrcc.dri.edu/cgi- bin/cliMAIN.pl?mt1047 accessed. 28/03/2017.
Wilson, H.F., Xenopoulos, M.A., 2009. Effects of agricultural land use on the composition of fluvial dissolved organic matter. Nat. Geosci. 2, 37–41.
Wu, F.C., Tanoue, E., Liu, C.Q., 2003. Fluorescence and amino acid characteristics of molecular size fractions of DOM in the waters of Lake Biwa. Biogeochemistry 65, 245–257.
Zhao, A., Zhang, M., He, Z., 2012. Characteristics of soil water-soluble organic C and N under different land uses in Alaska. Soil Sci. 177, 683–694.
Zhou, Y., Shi, K., Zhang, Y., Jeppesen, E., Liu, X., Zhou, Q., Wu, H., Tang, X., Zhu, G., 2017. Fluorescence peak integration ratio I_C:I_T as a new potential indicator tracing the compositional changes in chromophoric dissolved organic matter. Sci. Total Environ. 574, 1588–1598.
Zsolnay, Á., Baigar, E., Jimenez, M., Steinweg, B., Saccomandi, F., 1999. Differentiating with fluorescence spectroscopy the sources of dissolved organic matter in soils subjected to drying. Chemosphere 38, 45–50.